European Journal of Immunology

Nanoemulsion mucosal adjuvant uniquely activates cytokine production by nasal ciliated epithelium and induces dendritic cell trafficking

Paul E. Makidon[1,2,3], Igor M. Belyakov[1,3], Luz P. Blanco[3], Katarzyna W. Janczak[1,3], Jeffrey Landers[1,3], Anna U. Bielinska[1,3], Jeffrey V. Groom II[1,3] and James R. Baker Jr.[1,3]

[1] Division of Allergy and Clinical Immunology, Internal Medicine, University of Michigan, Ann Arbor, Michigan, USA
[2] Unit for Laboratory Animal Medicine, Medical School, University of Michigan, Ann Arbor, Michigan, USA
[3] Michigan Nanotechnology Institute for Medicine and Biological Sciences, University of Michigan, Ann Arbor, Michigan, USA

While the nasal mucosa is a potentially useful site for human immunization, toxin-based nasal adjuvants are generally unsafe and less effective in humans. Safe mucosal adjuvants that activate protective immunity via mucosal administration are highly dependent on barrier antigen sampling by epithelial and DCs. Here, we demonstrate that protein antigens formulated in unique oil-in-water nanoemulsions (NEs) result in distinctive transcellular antigen uptake in ciliated nasal epithelial cells, leading to delivery into nasal associated lymphoid tissue. NE formulation also enhances MHC class II expression in epithelial cells and DC activation/trafficking to regional lymphoid tissues in mice. These materials appear to induce local epithelial cell apoptosis and heterogeneous cytokine production by mucosal epithelial cells and mixed nasal tissues, including G-CSF, GM-CSF, IL-1a, IL-1b, IL-5, IL-6, IL-12, IP-10, KC, MIP-1a, TGF-β, and TSLP. This is the first observation of a nasal adjuvant that activates calreticulin-associated apoptosis of ciliated nasal epithelial cells to generate broad cytokine/chemokine responses in mucosal tissue.

Keywords: Adjuvants · Cytokines · DCs · Epithelial cells · Mucosal vaccines


Supporting Information available online

Introduction

The respiratory mucosa is the main port of entry for many important human pathogens including influenza, adeno, corona, rhino, and respiratory syncytial viruses, *Mycobacteria tuberculosis*, *Streptococcus pneumoniae*, and others. The nasal cavity is the first anatomical interface between these airborne microorganisms and the airway mucosa [1]. Recent evidence points to the concept that early events in nasal pathogen invasion and the penetration of microbes beyond the nasal submucosa are critical for the induction of innate and adaptive immune responses [2]. Given this, it therefore would be valuable to generate a protective, long-lasting immune response against pathogens at mucosal surfaces. Despite this, challenges to effective mucosal vaccination include difficulties in generating effective mucosal immunity, and the lack of safe, effective mucosal adjuvants and delivery systems.

Correspondence: Dr. Paul E. Makidon
e-mail: pmakidon@umich.edu

The transport of antigens across the nasal epithelial barrier is the first step in the induction of a mucosal immune response, and antigen sampling in this process is influenced by a number of factors. Entry of antigens or microbial pathogens into the mucosal epithelium is dependent on molecular interactions between the surface of the foreign material with host cell receptors that include complex glycoproteins, proteoglycans, and glycolipids [3, 4]. Innate mucosal cells, such as macrophages, DCs, and respiratory epithelial cells identify dangerous microorganisms through the recognition of specific pathogen-associated molecular patterns including Toll-like receptors (TLRs), NOD-like receptors, retinoic acid inducible gene I-like helicases, and C-type lectins [5]. Translocation of particulate antigens, intact bacteria, or viruses from the upper airways to APCs, is believed to occur mainly in nonciliated microfold cells (M-cells) [6, 7] that are located in specialized tissues such as the Waldeyer's ring in humans and nasal-associated lymphoid tissue (NALT) in rodents [8]. However, nonsoluble antigen uptake can occur in sinonasal ciliated epithelial cells by infection [9]. TLR-activated DCs ($CD11c^+$ $CX3CR1^+$ DCs) residing in the baso-lateral side of gut mucosal tissues extend processes across the tight junctions between epithelial cells and are also capable of capturing pathogens [10]. It remains, however, unclear how this process occurs in the nasal mucosa although direct luminal sampling by DCs is likely in areas of nasal stratified squamous epithelia where no directional transcytosis is thought to occur [11].

Several micro- and nano-polymeric vaccine delivery systems have been developed and do not activate immune cells but protect antigens from proteases in the mucosa. These materials appear to enhance antigen uptake through transcytosis in nonciliated epithelium or M-cells, but the induction of robust or protective immunity with these materials often requires the addition of inflammatory compounds [12].

Experimental mucosal adjuvants containing TLR agonists can stimulate innate immune responses and promote protection against pathogen challenge [13, 14]. An adjuvant system utilizing TLR signaling approved for human use is included in Cervarix (GlaxoSmithKline) that is a combination of alum and Monophosphoryl Lipid A (a TLR 4 ligand) [15]. In addition, enterotoxin-based adjuvants, such as cholera toxin (CT) and *Escherichia coli* heat-labile toxin (LT), which produce Th2-biased immune responses [16] to coadministered antigens have been shown to effect antigen trafficking when administered intranasally [17]. However, although CT and LT enhance antigen sampling, they also induce inflammation though ADP-ribosyltransferase activity that permeabilizes the nasal epithelium, and this allows entry of vaccine proteins into olfactory tissues. This limits clinical use because of toxicity and potential brain and peripheral nerve inflammation [18, 19]. Thus, no nasal adjuvant has been fully effective and safe for use in human vaccines and further development nasal adjuvants requires a better understanding of the mechanisms that promote innate immunity [20, 21].

The following studies were designed to evaluate the mechanism of adjuvant activity of a novel soybean oil-in-water nanoemulsion (NE) nasal mucosal adjuvant. NE is unique in that it induces immune responses in the absence of histological nasal inflammation [22–25]. When mixed with protein antigens, NEs promote robust mucosal immunity; high serum antibody titers; and a cellular immune response consisting of Th1, Th2, and Th17 responses [22, 23, 26]. We found that NE immune induction in ciliated epithelial-cells appears to mimic some aspects of respiratory viral infection in the nasal epithelium. It indicates that NE nasal adjuvant induces unique immunomodulatory and antigen trafficking activities that are different from toxin-based adjuvants and demonstrate novel activities associated with immune potentiation in the nasal mucosa.

Results

NE promotes mucosal antigen uptake and trafficking to regional draining lymph nodes in vivo

To determine if the NE mucosal adjuvant is capable of enhancing antigen uptake, cytokine production, and DC trafficking to regional lymph nodes, we first sought to evaluate NE's capacity to enhance internalization of antigen after exposure in vivo. Quantum dots (QDOTs, nondegradable nanometer-sized crystalline particles composed of cadmium selenide and surface modified to reduce nonspecific interaction) were used as surrogate antigen and nasally administered in live outbred CD-1 mice in the presence or absence of 20% NE. The distribution of QDOT-specific fluorescence was imaged at 18 h (Fig. 1A). Significantly more fluorescence was observed at this time point in the nose, cervical, and mediastinal LN regions following nasal administration of NE-QDOTs as compared with that of QDOTs administered in PBS. This suggested enhanced uptake of QDOTs in regional lymphatic tissues after administration in NE.

To further characterize the distribution of protein antigens after nasal administration in NE, 10 μg of GFP (used as a model, protein antigen) was administered intranasally to CD-1 mice in the presence of 20% NE. As shown in Fig. 1B, 18 h following nasal exposure, more fluorescence was detected throughout the nasal epithelium (a mixture of epithelium, connective tissues and lymphocytes, cervical LN, and mediastinal LN in GFP-NE treated mice than in mice exposed to GFP alone). GFP fluorescence was broadly distributed through the epithelial barrier after nasal inoculation with NE. These data corroborated the QDOT whole body distribution findings.

NE-mediated antigen uptake in the organized nasal-associated lymphoid tissue

Nasopharyngeal M-cells are implicated in particulate antigen sampling in nasal compartments in mice. We therefore qualitatively evaluated NALTs (a mixture of epithelial cells, connective tissues, and lymphocytes) [27] for the presence of GFP 18 h following

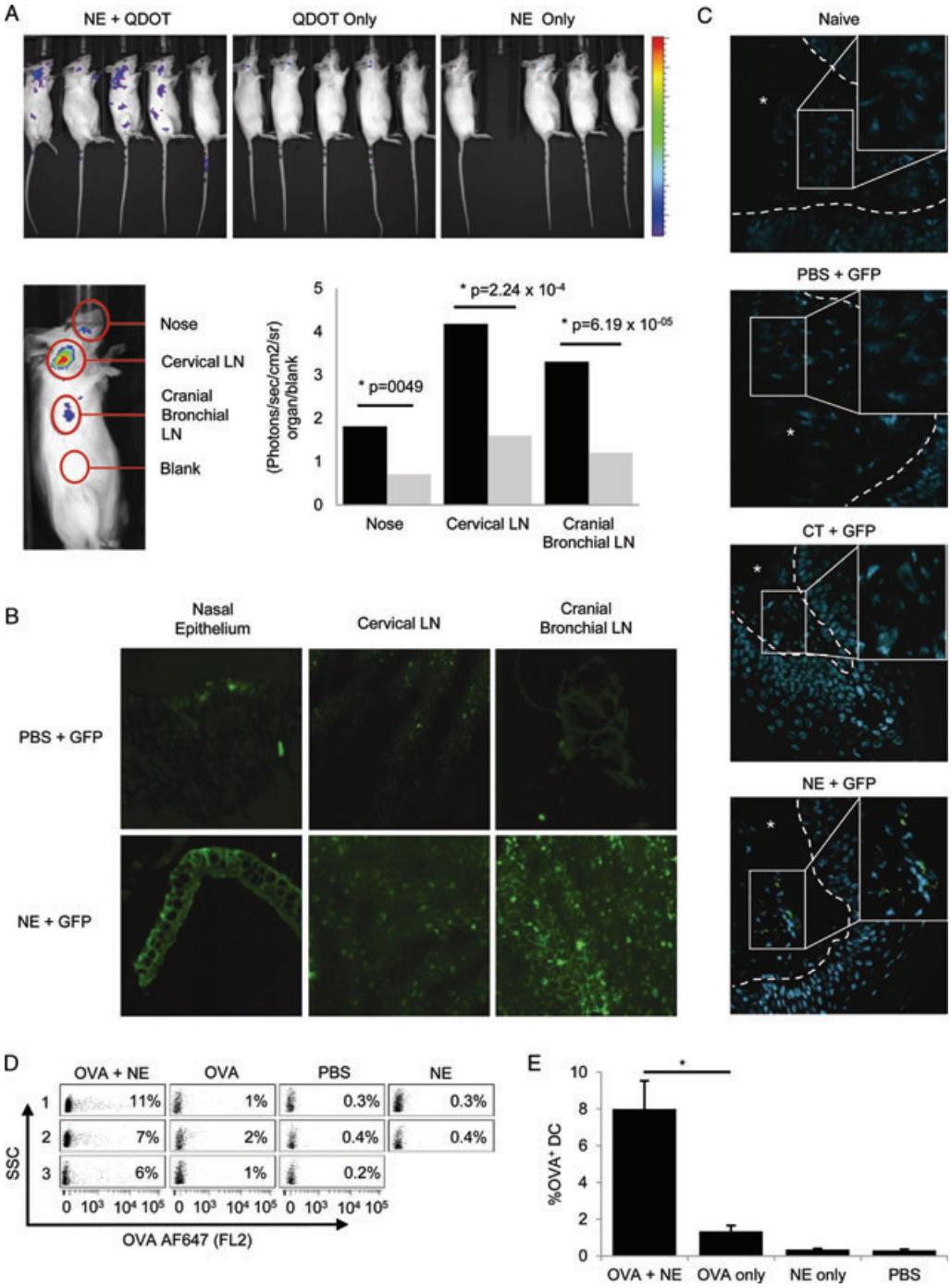

Figure 1. NE promotes mucosal antigen uptake and trafficking to regional lymphoid tissue. (A) CD-1 mice were treated with QDOTs mixed with NE, QDOTs in PBS, or 20% NE alone. In vivo fluorescence was measured at 18 h. The mouse furthest to the right in each group is a nontreated control. Black bars: NE + QDOT, gray bars: QDOT only. *$p < 0.05$ Mann–Whitney test. Data are shown as mean of five mice per treatment and experiments were performed twice with comparable results. (B) In situ fluorescent evaluation of the indicated cryo-preserved tissues in CD-1 mice 18 h following instillation of 7.5 μL/nostril of GFP (10 μg) either diluted in PBS or mixed with 20% NE. Magnification is 400×. Data shown are representative of experiments performed on three mice per treatment, and repeated twice with comparable results. (C) In situ fluorescent evaluation of the NALT in naïve CD-1 mice or 18 h following instillation of 6 μL/nostril of GFP (10 μg) alone or in combination with 1 μg CT or 20% NE. Tissues were evaluated with confocal microscopy; 400× magnification. Insets represent 800× magnification of the indicated boxed regions. The dashed white line marked with an asterisk demarks the area of the subepithelial dome. Data shown are representative of experiments performed on three mice per treatment and repeated twice with comparable results. (D) NALT cells (1–2 × 10^6/sample) isolated from CD-1 mice 36 h following nasal treatment with 10 μg OVA-Alexa 647 ± 20% NE (10 μL/nostril) or 20% NE alone (10 μL/nostril) were analyzed for OVA-Alexa 647 uptake. Numbers represent the percentage of cells that have internalized OVA-Alexa 647 among $CD11c^+$ lymphocytes based on CD11c gating. Data shown are representative of experiments performed on three mice per treatment, and repeated twice with comparable results. (See gaiting strategy in Supporting Information Fig. 1). (E) Quantitative analysis of OVA^+ DCs expressed in (D) as a percentage of total cells in NALTs + STD). *$p = 0.0058$, Unpaired Student's *t*-test.

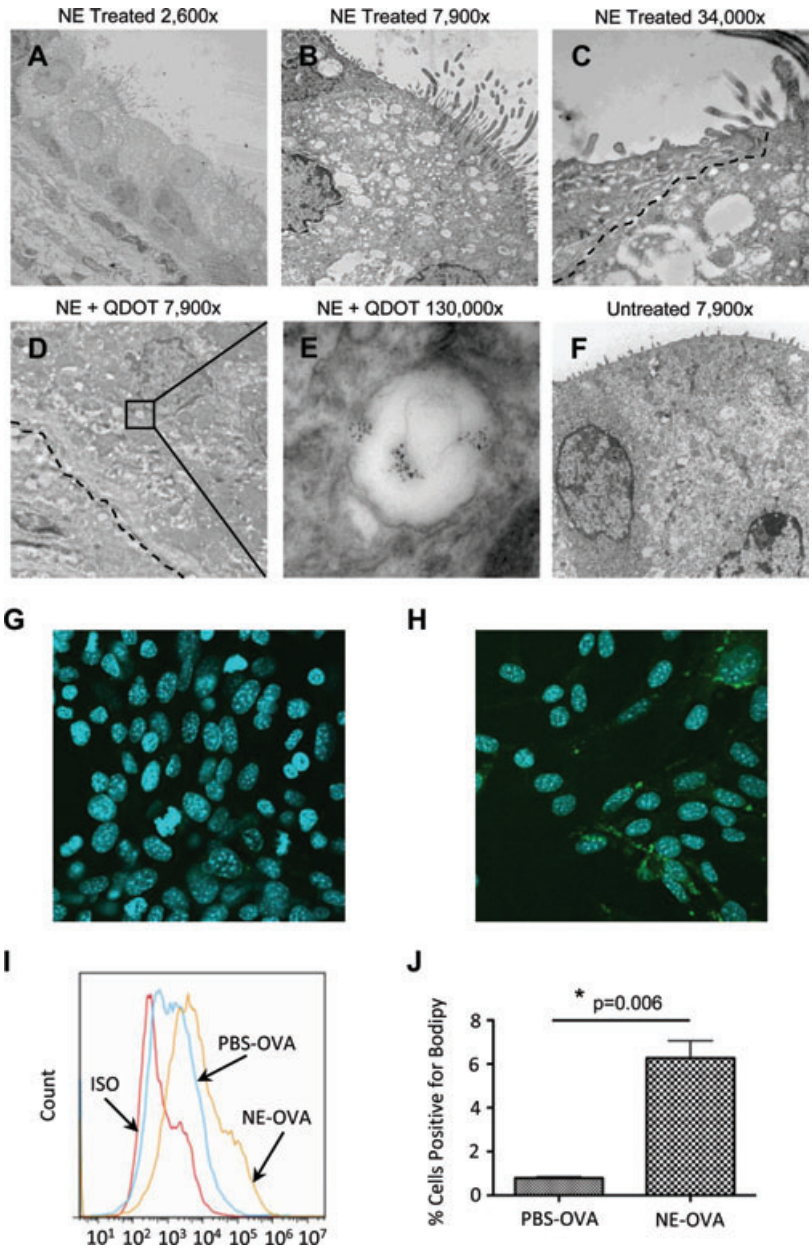

Figure 2. NE promotes in vivo sampling by ciliated nasal epithelial cells without disruption of the epithelial barrier. TEM images of nasal epithelium from CD-1 mice 18 h after nasal inoculation with QDOTs: images of epithelium following 20% NE treatment (7.5 μL/nostril) (A–E). The dashed line in (C) highlights the tight junction between adjacent epithelial cells. (D and E) Epithelium following intranasal inoculation with QDOTs mixed with 20% NE. The dashed line in (D) demarks the basal lamina. (E) Represents an expansion of the boxed area in (D). (F) An image of control (nontreated) nasal epithelium. The magnification of each section is listed above the photomicrograph in (A–F). Data shown are representative of experiments performed on three mice per treatment and repeated twice with comparable results. (G–H) Intracellular BODIPY fluorescence (green) associated with DQ-OVA uptake and processing in TC-1 epithelial cells exposed to (G) DQ-OVA without adjuvant or (H) a mixture of NE and DQ-OVA. The blue fluorescence represents DAPI nuclear stain. Data shown are representative of two experiments performed with comparable results. Magnification is 400×. (I) Flow cytometry analysis of DQ-OVA uptake in primary nasal septal epithelial cells. Single-cell suspension of primary nasal septal cells (1×10^6/sample) isolated from C57bl/6 mice 2 h following nasal treatment with 4 μg DQ-OVA ± 0.1% NE (orange histogram) or 4 μg DQ-OVA alone (blue histogram). The red histogram indicates the isotype control. Data shown are representative of two experiments performed with comparable results. (J) The percentage of cells containing processed DQ-OVA is presented as mean ± SEM of three samples per treatment and are representative of two experiments. *Indicates statistical significance as analyzed by unpaired Student's t-test.

nasal administration (Fig. 1C) of either NE-GFP (bottom panel), CT-GFP (third panel down), GFP only (second panel down), or naïve mice (top panel). GFP was identified in the subepithelial dome and along the luminal border in mice treated with GFP-NE but not in mice treated with GFP in saline. Interestingly, GFP was not detected in significant amounts in GFP-CT immunized mice at that time point. The considerable presence of GFP in the NALT in NE-GFP immunized mice suggests that NE also serves as a depot promoting longer retention of the protein in the mucosa in comparison with CT. This was confirmed by flow cytometry, where we observed a significant increase ($p = 0.007$) in OVA-Alexa 647 in $CD11c^+$ NALT-isolated cells in NE-treated mice compared with those from naïve mice (Fig. 1D and E and Supporting Information Fig. 1).

NE-mediated transcellular antigen uptake in ciliated epithelial cells

As indicated in Fig. 1B, NE-facilitated antigen uptake may not be completely explained by APC sampling. Transmission electronic microscopy (TEM) was employed to characterize the subcellular distribution of NE-antigen in nasal mucosa 18 h after administration of QDOTs in NE in situ (Fig. 2A–F). We found that ciliated cells (identified morphologically) contained vesicle-like material homogenously distributed throughout the cytoplasm (Fig. 2A–C). These vesicle-like structures appeared to be in endosomes [28] and not apoptotic bodies [29] and had an average diameter of 0.479 microns consistent with the size of NE droplets. The QDOT-like material present in the vesicle-like structure measured on average

5 nm. Tight junctions in these cells remained intact despite the lipid inclusions (Fig. 2C, dashed line) and, epithelial cells from control mice had no cytoplasmic lipid structures (Fig. 2F). Under higher magnification (Fig. 2D and E), QDOTS were detected in vesicles and in the cytoplasm proximal to the basal lamina (Fig. 2D, dashed line) indicating the material stayed with the NE (Fig. 2E). NE-facilitated epithelial cell antigen uptake was confirmed in vitro using TC-1 cells (a murine respiratory epithelial cell line) and in purified cultures of primary nasal septal epithelial cells [30] collected from naïve adult C57BL/6N mice. Uptake of antigen was analyzed by confocal microscopy in TC-1 and by flow cytometry in primary nasal septal epithelial cells exposed to a mixture of NE and ovalbumin labeled with fluorescent dye BODIPY (DQ-OVA). Cells exposed to the mixture of NE and DQ-OVA (Fig. 2H) had more intracellular BODIPY than did those cells exposed to DQ-OVA alone (Fig 2G). Uptake was significantly higher ($p = 0.006$) in primary epithelial cultures treated with NE + DQ-OVA as compared with that of cells exposed to DQ-OVA without NE (Fig. 2I and J).

NE mediates inflammation via calreticulin-associated epithelial cell apoptosis and necrosis

We sought to determine the relevance of NE-facilitated antigen uptake in ciliated epithelial cells for APC-associated antigen trafficking. We hypothesized that NE-loaded epithelial cells undergo apoptosis or necrosis, and are then sampled by DCs. To evaluate this, nasal epithelium (a mixture of columnar epithelium, connective tissues, and lymphocytes) was harvested from mice 2 h following exposure to 15 μL 20% NE or its components (cetylpyridinium chloride (CPC) or NE without CPC ($W_{80}5E$)). The epithelium was evaluated in situ for apoptosis by staining for caspase-3 and by examining morphology for necrosis (Fig. 3A). Both caspase-3 expressing apoptotic (red arrows) and necrotic cells (black arrows) were identified in NE-treated epithelium (Fig. 3A, lower left panel), and these changes occurred without significant cellular inflammation. In contrast, tissues from mice treated with CPC alone underwent severe necrotic changes (upper right panel) with areas of complete epithelial disruption associated with neutrophil infiltration (green arrows). Interestingly, mice treated with NE without CPC (Fig. 3A, lower right panel) had similar architecture in comparison with that of PBS-treated controls (Fig. 3A, upper left panel), suggesting a role for CPC in the induction of apoptosis. Both the apoptotic and the necrotic processes associated with NE were associated with limited, focal disruption of tight junctions thus allowing para-cellular antigen infiltration into the epithelium. To further characterize the apoptosis, nasal epithelial tissue sections were probed for calreticulin, an ectopically exposed protein expressed by cells undergoing immunogenic cell death [31]. As shown in Fig. 3B lower left panel, the epithelium from NE-treated mice showed markedly positive staining for calreticulin that was not observed in the epithelia from control animals (Fig. 3B, upper left, upper right, and lower right panels). These results suggest that NE uniquely induces immunogenic epithelial cell apoptosis

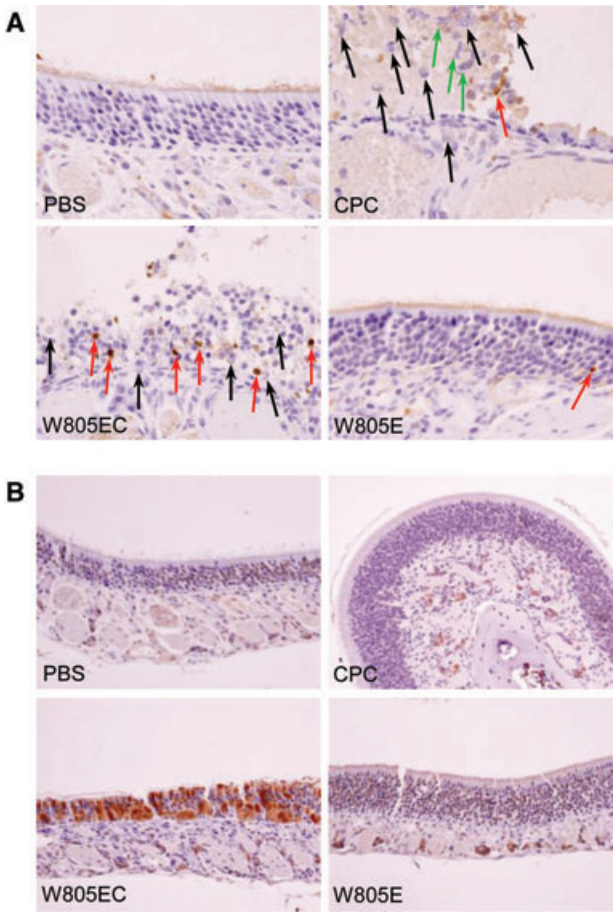

Figure 3. NE stimulates calreticulin-associated epithelial cell apoptosis and necrosis. (A) Nasal respiratory epithelium was harvested from 10-week old female C57BL/6N mice 2 h following treatment with 15 μL 20% NE or its components; CPC or NE without CPC ($W_{80}5E$). Dark brown inclusions indicate caspase-3 staining (red arrows). Necrotic cells are indicated by black arrows. Neutrophils are indicated with green arrows. Magnification is 400×. (B) The nasal epithelium was probed for calreticulin expression. Cells taking up stain for calreticulin appear dark brown in color. Magnification is 200×. Data shown are representative of two experiments performed, each with three mice per treatment, with comparable results.

that could stimulate APC activity and mediate the generation of immunity.

NE stimulate accessory antigen presenting activity of nasal epithelial cells

To analyze NE-induced local epithelial gene expression, whole nasal mucosal tissue were harvested 6 and 24 h following nasal instillation of 20% NE (15 μL) in healthy adult outbred CD-1 mice as described in the *Materials and methods* (Complete microarray data have been deposited in the public database Gene Expression Omnibus (GEO) under series accession number GSE25486). Hierarchal cluster analysis of the expression of genes related to antigen processing and presentation was performed on the nasal mucosa using the GO term 0006955 Immune Response (Fig. 4A). Upregulation of MHC class I and II transcripts and

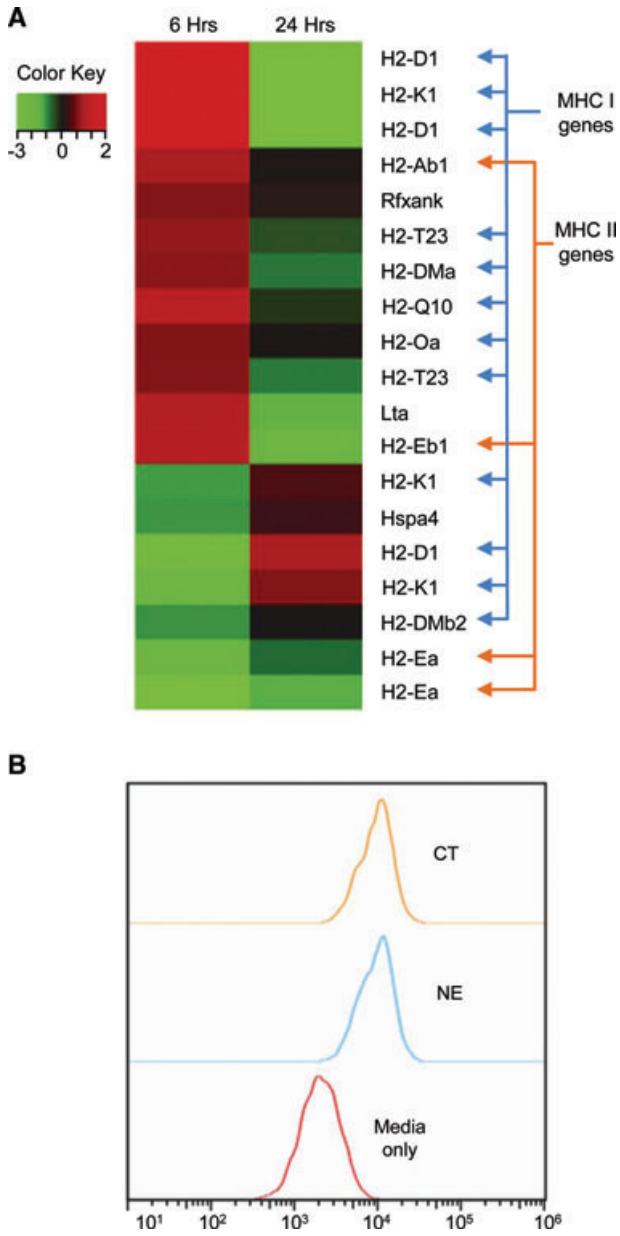

Figure 4. NE-modulated MHC class I and class II gene expression in nasal mucosa. (A) Hierarchal cluster analysis of antigen processing and presentation pathway gene expression in CD-1 mouse nasal mucosa 6 or 24 h following exposure to 20% NE (7.5 μL/nostril). Gene regulating expression of MHC class I or class II is indicated by the blue or orange arrows, respectively. The colors represent significant ($p < 0.05$ and fold change >2 over control tissue) changes in gene expression (Red: upregulated and green: downregulated). Gene expression data are representative of two independent experiments each using three mice per treatment. (B) MHC class II surface expression in primary nasal epithelial cells. A total of 1×10^6 nasal epithelial cells harvested from C57BL/6N mice were treated with either 0.0001% NE, 10 μg CT, or media alone for 12 h. The cells were probed for MHC class II expression and analyzed via flow cytometry. MHC class II expression on primary epithelial cells untreated (red histogram), NE-treated cells (blue histogram), and CT-treated cells (orange histogram). MHC class II flow cytometry data are representative of at least six independent experiments.

multiple other antigen presentation accessory molecules were observed in the nasal mucosa at 6 and 24 h in NE exposed mice.

To determine if these NE activities enhance MHC class II expression in nasal epithelial cells, purified cultures of primary nasal septal epithelial cells [30] were harvested from adult C57BL/6N mice and probed for surface expression of MCH class II after treatment with NE (0.0001%) and compared with treatment with cells exposed to 10 μg/mL CT for 12 h or media alone as controls (Fig. 4B). NE induced significantly more expression of MHC class II in comparison with the control groups ($p = 6.3 \times 10^{-5}$) similar to that which was observed with CT ($p > 0.05$).

DEC205$^+$ DCs traffic NE-associated antigen to the cervical LN

We also examined the phenotype of APCs associated with NE-GFP in the superficial cervical LN, by examining colocalization of GFP with DEC205, CD19, or CD11b using laser confocal microscopy. Eighteen hours following the administration of 10 μg GFP ± 20% NE (15 μL), GFP was observed to localize in DEC205$^+$ cells but not in CD19 or CD11b expressing cells in the cervical LN (Fig. 5 and

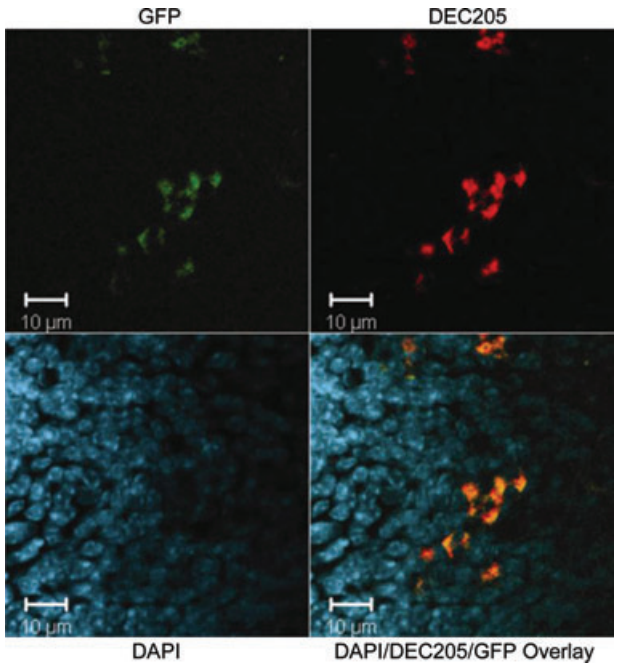

Figure 5. NE adjuvant promotes in vivo GFP localization in cells expressing DEC205. Colocalization of GFP (green) and DEC205 surface markers (red) in the cervical LNs of CD-1 mice 18 h after nasal treatment with 13 μg GFP plus 20% NE (15 μL). The photomicrograph in the upper left corner represents GFP. The photomicrograph in the upper right corner represents red channel fluorescence (DEC205). The photomicrograph in the lower left corner represents ultraviolet channel fluorescence (DAPI). The photomicrograph in the lower right corner represents the overlay image of all of the channels. Scale bar: 10 μm. Data shown are representative of two experiments performed, with comparable results.

data not shown). These results indicate that mature DCs efficiently traffic NE-associated antigen to regional LN following nasal NE-antigen administration.

Innate and adaptive immune responses after NE or CT stimulation in vivo

To define NE-specific effects on the innate cytokine profile of nasal tissue, RNA from isolated nasal mucosa (a mixture of epithelial cells, connective tissues, and lymphocytes) was harvested following administration of 20% NE (15 μL) in healthy adult CD-1 mice. Microarray analysis showed 2968 (1975 upregulated and 993 downregulated) changes in gene expression at 6 h versus animals receiving PBS (complete microarray data have been deposited in the Gene Expression Omnibus (GEO) data base under series accession number GSE25486). These data were analyzed for immune-related genes (KEGG term cytokine–cytokine interaction (04060)), and expression of only 22 genes (10.5%) showed significant increases at 6 h after nasal treatment with NE. RNA transcripts from the pro-inflammatory cytokines/chemokines GM-CSF, IL-1b, IL-6, KC, MCP-1, MIP-1α, RANTES, TNF, CXCL9, CXCL13 CXCL2, and CCL12 were significantly increased after exposure to NE.

Changes in protein concentration in homogenized nasal septal tissue collected from C57BL/6 mice treated with either NE or CT (and compared with that of PBS administration) were evaluated using a Luminex mouse 22-plex cytokine/chemokine kit and standard ELISA (Fig. 6A and C). Nasal treatment with 15 μL of 20% NE was associated with increases in the cytokines G-CSF, IL-1a, IL-5, IL-6, IL-12, IP-10, TGF-β, KC, and the DC maturation cytokine TSLP by 18 h. In contrast, the cytokine response profile of 1 μg of CT significantly differed from NE, with increases only in IL-6 and IL-12. The broader cytokine profile associated with the NE adjuvant includes both IL-6 and TGF-β, which relate to adaptive Th17 responses [26, 32].

While most studies evaluating adjuvant activity have focused on professional APCs we compared the cytokine profiles induced by NE in both epithelial cells and APCs given the ciliated epithelial cell data presented above (Fig. 2). This was done by stimulating bone marrow derived DCs (BMDCs) harvested from C57BL/6 mice with a range of either NE concentrations (0.001 to 0.1%) or CT (1 μg, 10 μg, or 30 μg). The cells were collected and evaluated for the presence of cytokines and chemokines using the Luminex assay described above (Fig. 6B and C). As compared with control cells, NE was found to stimulate significant production of four cytokines in supernatants from these cells including GM-CSF, IL-1α, IL-1β, and MIP-1α. CT also stimulated IL-1a, IL-1b, and MIP-1a in BMDCs in addition to 13 others including IP-10, G-CSF, IL-10, IL-4, IL-6, IL-9, IL-12, IL-15, IL-17, TNF-α, and KC; therefore the profiles were very different. Interestingly, the only NE-stimulated cytokine significantly increased in both the nasal septum and BMDCs was IL-1α.

To validate these results, TC-1 epithelial cells were incubated in media with either NE or CT as above. The supernatant from treated cells were evaluated with ELISA for IL-6, TGF-β, and TSLP (Fig. 6A and C). Significant amounts of IL-6, TGF-β, and TSLP were measured in supernatant collected from cells incubated with NE; however, only IL-6 was induced in response to CT. Collectively, this data indicate that NE uniquely promotes innate cytokine and chemokine activity in epithelial cells in addition to activating APCs.

Evaluation of the role of the IL-6 cytokine in the adjuvant activity of NE

IL-6 is significantly produced in the nasal mucosa after exposure to NE, but the exact role of IL-6 in the acute phase response in the nasal mucosa is poorly understood [33]. To characterize its role NE-induced immunity, we immunized mice deficient in the ability to produce IL-6 (IL-$6^{-/-}$) with 20% NE + 20 μg rPA and compared rPA-specific splenocyte responses from $IL6^{-/-}$ and WT mice (Table 1). IL-5 cytokine secretion trended higher in the IL-$6^{-/-}$ mice while IFN-γ, TNF-α, and IL-17 trended lower. Thus, these results suggest that IL-6 plays an important cytokine in NE-mediated immune activation in the nasal respiratory mucosae.

Discussion

Previous studies have documented that intranasal immunization with high-energy NEs and either whole organism or recombinant proteins induces a broad and unique immune response [23, 26, 34, 35]. However, the mechanisms of NE adjuvant activity are still unknown and this hinders the development of these adjuvants. In addition, enhancing the knowledge into the mechanisms of action of other mucosal adjuvants, including CT, also will aid in the rationale design of improved adjuvant formulations. The present study examines novel NE adjuvant activities involving uptake of antigen and immunoregulatory cytokine production by ciliated nasal epithelial cells in the absence of inflammation in comparison with CT. We also examined the effects of NE on antigen internalization in nasal mucosa, its uptake by APCs and subsequent trafficking to draining lymph nodes. Several unique activities were observed.

Our current studies document that NE not only enhanced antigen uptake in the NALT but also, for the first time, we demonstrate enhanced uptake in ciliated epithelial cells using a mucosal adjuvant (Fig. 1). The presence of emulsion droplets containing QDOTs in ciliated epithelial cells (Fig. 1D and E) suggests that the cells internalize this material through a process that does not disrupt tight junctions or cell membranes. These results also suggest that nasal mucosa NE antigen uptake does not require M-cell or DC luminal sampling. This unique route of facilitated antigen uptake in nasal tissues appears to be transcellular as opposed to para-cellular as evidenced by the finding that tight-junctions remain intact despite the presence of NE (Fig. 1C). Furthermore, no disruptive changes or inflammation were observed in the epithelial layer on either the EM images or with light microscopy [23]. Together, these data suggest that NE is able to induce unique systemic immune responses through a new pathway for antigen uptake leading to DC migration from mucosa to systemic lymphatic tissues.

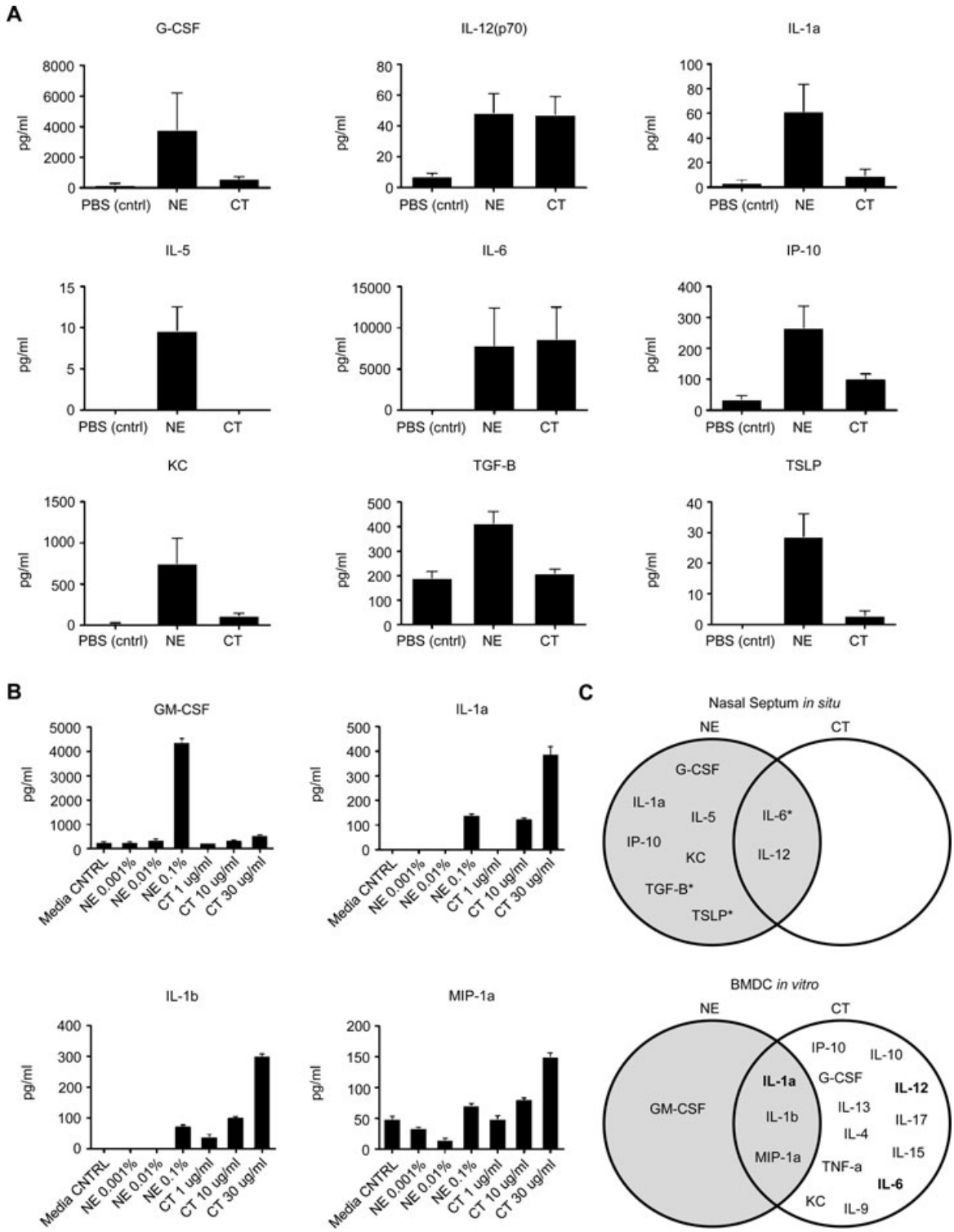

Figure 6. NE has unique immunomodulatory function in respiratory mucosa. (A) Immunodetection of NE-driven, mucosally secreted innate cytokines and chemokines after intranasal treatment with NE. Cytokine and chemokine secretion in homogenized nasal septal tissues collected from C57BL/6N mice 18 h following intranasal administration of 20% NE (7.5 μL/nostril), or 1 μg CT (7.5 μL/nostril), or PBS (7.5 μL/nostril). Protein detection is expressed in group average protein concentration in pg/ml + SEM of three mice per treatment and data are representative from two experiments. (B) Immunodetection of cytokines and chemokines in BMDCs. A total of 4×10^6 BMDCs ($n = 3$ cultures/treatment) were stimulated with 0.001%, or 0.01% or 0.1% of NE, or 1 μg/mL, or 10 μg/mL or 30 μg/mL of CT for 24 h. Protein detection is expressed in group average protein concentration in pg/mL + SEM. This assay was repeated twice for verification. The data are representative of 1 of the 2 experiments performed with comparable results. (C) VENN diagram comparing the NE-specific versus CT-specific profiles of cytokines and chemokines in nasal mucosa versus BMDCs. *Validated NE-specific production in TC-1 epithelial cells. Data were analyzed by unpaired Student's *t*-test.

Table 1. Cytokines produced by splenocytes from IL-6$^{-/-}$ or WT mice with NE + rPA following stimulation with rPA in vitro

Splenocyte-derived cytokines	Fold antigen specific stimulation[a)]	
	IL-6$^{-/-}$	WT
Th1 type		
IFN-γ	1 (0.1)	37.09 (3.71± 3.13)
TNF-α	1 (0.1)	142.9 (14.29 ± 7.43)
IL-2	8.75 (67.3 ± 47.53)	2.97 (37.39 ± 14.28)
Th2 type		
IL-6	1.09 (5.58 ± 0.85)	2.38 (30.2 ±10.9)
IL-4	78.5 (7.85 ± 6.71)	9.36 (7.84 ± 3.37)
IL-5	308.57 (175.89 ± 146.39)	14.19 (51.28 ± 26.02)
IL-10	2.86 (21.03 ± 12.22)	1.52 (50.17 ± 15.32)
Th17 type		
IL-17	39.14 (3.91 ± 3.3)	2.88 (58.61 ± 25.39)

[a)] Shown are the averages of ratio (stimulation plus rPA/stimulation with media without rPA) for four different mice. The numbers in parenthesis represent absolute values in pg/mL ± SEM. Cytokines were detected by Luminex assay as explained in the section Materials and methods.

The ability of NE to promote transcellular antigen uptake may be related to "lipidizing" proteins to enhance transcellular absorption in respiratory epithelial barriers. Mixing antigen with NE appears to trap the antigen in the oil phase [23] allowing transcellular migration across the apical membrane, through the cell cytoplasm, and across the basolateral membrane. This is the main route of permeation for hydrophobic compounds across the mucosa and is very efficient given the surface area of the transcellular approach is much larger by a factor of 9999 to 1 than the surface area of the para-cellular route (tight junctions) [36, 37]. Also, the finding that lipid droplets penetrating the nasal mucosa induce Th1, Th2, and Th17 type of immune response may suggest that this system evolved to deal with lipid-covered respiratory viruses, especially since the emulsion droplets are approximately the same size as viruses, are highly surface active, and readily endocytosed by epithelial cells.

Following epithelium cell uploading of the NE-antigen complex, DEC205$^+$ cells appear to locally sample antigen in the epithelia and then migrate to the systemic lymphatic circulation (Fig. 5). Optimal conditions and regulations of initial antigen sampling and activation of DCs causing migration to draining lymph nodes is not very well understood at this moment. We found that some NE and antigen-loaded epithelial cells undergo calreticulin-associated apoptosis and necrosis (Fig. 3). DCs most likely take these antigen-loaded dead cells up. We hypothesize that host DNA released from dying cells may act as a damage-associated molecular pattern that mediates DC activation, potentially in a similar fashion as has been reported for alum [38]. It is also possible that there is direct interaction between NE and antigen-loaded ciliated epithelial cells and antigen-specific CD4$^+$ and CD8$^+$ cells in sinonasal epithelium. This hypothesis seems plausible given the fact that NE stimulates accessory antigen processing and presentation activities by MHC class I and II in epithelial cells (Fig. 4). Finally, the possibility that epithelial cells secrete biologically active exosomes capable of uptake by DCs or presenting antigenic peptide in the context of MHC class I or class II to naïve T cells merits further investigation [39, 40]. Any of these processes could activate DCs and account for lymphatic migration.

Nochi and colleagues have demonstrated that nanogel, when applied intranasally, activates cytokine production and generates cellular immune responses [41]. The majority of mucosal adjuvants cause local inflammation that attracts and activates antigen-presenting cells through cytokines, chemokines, and multiple signaling pathways such as MyD88 [42, 43]. This microenvironment facilitates local antigen sampling by DCs and enhances presentation to the immune system after toxin administration. However, our findings suggest that the mechanisms of NE adjuvant activities appear to be distinctive from that of CT (Fig. 6) and possibly other nasal adjuvants. This is supported by the unique and heterogeneous production of cytokines and the absence of histological inflammation [23].

In these studies, we demonstrated that NE induces a cytokine profile that supports antigen-specific adaptive Th17 responses. In the intestinal mucosa, Th17 cells are the main source of IL-17, whereas in the respiratory mucosa γδT cells, NKT, NK, RORγt, and NKp46$^+$ cells are the main producers of IL-17. Effector antibacterial and antifungi functions of IL-17 are attributed to the interaction with IL-17R expressed on fibroblasts and epithelial cells to induce MCP-2, G-CSF, and CXC chemokines. IL-22 is another important cytokine produced by Th17 for inducing the secretion of antimicrobial peptides and β-defensin-2 by epithelial cells and for contributing to barrier function and tissue repair [44]. Beyond its role in the Th17 pathway, IL-6 also enhances innate immunity and antibody production following mucosal vaccination [45, 46]. IL-6 may actually be muco-protective, downregulating TNF and IL-1 [47, 48] and has been shown to enhance transcellular passage of microbes through the epithelial barrier. The exact mechanism of epithelial cell production of IL-6 in response to NE exposure requires further investigation.

In the future, the development of mucosal vaccines against infectious diseases will necessitate the development of safe and effective mucosal adjuvants and delivery systems. In these studies, we demonstrate NE-mediated antigen uptake into ciliated epithelium that facilitates DC antigen loading and migration to mucosal and systemic lymphatic tissues. NE also uniquely enhanced heterogeneous cytokine and chemokine production by epithelial cells. These responses may have a significant role in inducing protection against bacterial, viral, and fungi infectious.

Materials and methods

Mice

CD-1® and C57BL/6N mice were purchased from Charles River Laboratories (Wilmington, MA). IL-6 gene deficient mice (IL-6$^{-/-}$)

(B6.129S6-IL6^{TM1KOPF}) and C57BL/6J mice were purchased from Jackson Laboratories. All mice were housed in specific pathogen-free conditions in facilities maintained by the University of Michigan Unit for Laboratory Animal Medicine. The University Committee on Use and Care of Animals (UCUCA) at the University of Michigan approved all procedures performed on mice. In regards to characterization of humoral and cellular immune responses to NE-based vaccines, there have been no significant differences in response between strains, and the results observed in CD-1 mice also seen in C57BL/6 mice in previous studies.

Cell culture

Primary nasal epithelial cells were cultured from the nasal septum of C57BL/6N mice as previously described [30] with minimal exceptions. Purity was verified by probing for the lack of MHCII, CD11c, and CD11b. Mouse BMDCs were generated and maintained as described previously [49].

The murine pulmonary epithelial cell line TC-1 was obtained from ATCC (CRL-2785^{TM}) and cultured in RPMI 1640 containing L-glutamine (2 mM) supplemented with 10 mM HEPES, 1 mM sodium pyruvate, 100 μM MEM NEAA, 10% heat-inactivated FBS, 100 μ/ml Penicillin, and 100 μg/mL Streptomycin.

Nanoemulsions (NEs)

NEs were provided by NanoBio Corporation and obtained by nanoemulsification of Tween 80, CPC, ethanol as a solvent, highly purified soybean oil, and water.

Antigens

Enhanced GFP was acquired from BioVision Research Products. Alexa Fluor 647-conjugated OVA protein (OVA-Alexa 647) were purchased from Invitrogen^{TM}. Recombinant rPA from *Bacillus anthracis* were purchased from List Biological Laboratories, Inc. QDOTs (Qtracker 655 non-targeted) were purchased from Quantum Dot Corporation.

QDOT assay in vivo

QDOTs were used as a model antigen due to their high level of in vivo fluorescence and their ability to interact with the lymphoid tissues in the mice [50]. Groups of four mice were inoculated intranasally with 15 μL of QDOTs (6.6 μL of 2 μM solution, ±20% NE). In-life fluorescence analysis was performed in isoflurane-anesthetized mice using the IVIS Imaging System 200 Spectrum series bioluminometer (Xenogen). The fluorescent measurement was quantified using IVIS Living Image 3.1 software. Mouse no. 2 in the NE only treatment group died under anesthesia during the 4-h imaging time point. QDOT-specific fluorescent intensity is represented on an increasing scale from blue ($1. \times 10^7$), green (5×10^7), yellow, (7.5×10^7), and red (1×10^8) photons/s/cm^2/sr. The fluorescent measurement was quantified in the indicated regions and normalized to the signal collected from the blank on each mouse.

Antigen localization

To determine the localization of GFP antigen in different tissues 18 h after nasal vaccination, the mice were nasally immunized (15 μL/mouse) with a mixture of GFP (10 μg/mouse) ± NE (20%). The animals were sacrificed 18 h following inoculation, and nasal epithelium (a mixture of ciliated and nonciliated columnar epithelium, connective tissues, and APCs), superficial cervical lymph nodes, mediastinal lymph nodes, and organized NALTs [27] were collected in OTC (TissueTek) and frozen by slow immersion in liquid nitrogen. Tissue sections were cut in 5 μm sections and placed on glass slides for evaluation using light microscopy. NALTs were imaged with a Zeiss LSM501 laser confocal microscopy.

FACS analysis

Immunofluorescent studies of NALTs were confirmed using FACS. The presence of OVA-Alexa 647 was analyzed in single cell suspensions derived from NALTs of CD-1 mice 36 h following nasal immunization with 10 μg OVA-Alexa 647 ± 20% NE (15 μL/mouse). The cells were stained with APC hamster anti-mouse cD11c (BD Pharmingen^{TM}), rat anti-mouse cD19: Pacific Blue® (AbD serotec), PE anti-mouse cD11b (BioLegend), or their respective isotype. Samples were acquired using a LSR II (BD Biosciences). Data were analyzed on DIVA software (BD Biosciences). For these studies, we utilized the following gating strategy. Alexafluor 647$^+$ cells were identified in populations of CD11c$^+$ or CD11b$^+$ live cells based on side scatter versus CD11c or CD11b analysis.

FACS analysis of NE-inducible MHC class II expression in primary nasal epithelial cells

A primary culture of nasal septal epithelial cells was prepared as above. A total of 1×10^6 cells were incubated with 0.001 or 0.01 or 0.1 NE. Positive controls included 100 ng-500 ng LPS (*E. coli* K12) or 400 units of recombinant mouse TNF-a (Invitrogen). Negative controls included no treatment (media alone). The treated cells were washed, suspended in FACS buffer (Biolegend), and blocked on ice with TruStain fcX, Biolegend). The cells were then stained with 0.25 μg/10^6 cells of anti-I-A/I-E-alexa flour 647 (Biolegend) or isotype control for 20 min on ice. The cells were then washed twice and resuspended in FACS buffer prior to analysis via flow cytometer using a BD Accuri C6 Flow cytometer utilizing the following gating strategy. Based on analysis in a side and forward scatter plot, the dominant population (>95%) was analyzed for marker-specific signals.

Phenotype identification of NE-mediated APCs trafficking to draining lymph nodes

Superficial and deep cervical lymph nodes were harvested directly postmortem from CD-1 mice 18 h following treatment with GFP plus 20% NE (15 μL). The tissue was fixed in 10% buffered formalin and paraffinized. The tissue sections were blocked for 10 min using the Power Block® solution (BioGenex), and stained with anti-GFP fluorescent antibodies or control same isotype antibodies in PBS containing 0.1% BSA overnight at 4°C. Tissue was stained with the DC markers DEC205 (Rabbit anti-mouse CD205 mAb [Serotech]) and CD11c (rabbit anti-mouse cD11b [Abcam]) or macrophage marker cD11b. GFP was detected with mAb anti-GFP (rabbit pAb anti-GFP [Biosystems]). Goat anti-rabbit Dylight™ 594 (Biocare Medical) was used as a secondary antibody to rabbit primaries. The stained tissue samples were mounted in ProLong (DAPI blue nuclear stain Molecular Probes®). Imaging was performed using a Zeiss LSM501 laser confocal microscopy.

Electron microscopy of nasal epithelium

The sinus cavities were excised 18 h postinoculation and immersion fixed in 2.5% glutaraldehyde in 0.05 M cacodylate buffer, pH 7.4, at room temperature for 4 h. After fixation, the sections were demineralized in 7.5% disodium EDTA with 2.5% glutaraldehyde for 7 days following a protocol adapted from Shapiro et al. [51]. Ultra-thin sections were viewed without poststaining on a Philips CM100 at 60 kv. The images were recorded digitally using a Hamamatsu ORCA-HR digital camera system.

Antigen uptake and processing in epithelial cells in vitro

For uptake analysis in an epithelial cell line, 1×10^5 TC-1 cells were seeded in RPMI 1640 media (with L-glutamine; Mediatech, Inc.) with 10% heat-inactivated fetal bovine serum, 1% nonessential amino acids, 10 mM HEPES, 1 mM sodium pyruvate, 1% penicillin/streptomycin overnight at 37°C on Lab-tek chambered coverglass slides (Nunc). A mixture of DQ™ ovalbumin (DQ-OVA; Life Technologies) with 1:6 NE, or DQ-OVA alone was prepared in Dulbecco's PBS (DPBS; Life Technologies) at 10 times the desired final concentration, and added to the media in the cell chambers to achieve a final concentration of 0.012% NE and 2 mg/mL DQ-OVA. Samples were incubated for 1 h at 37°C. Media was removed, and cells were washed three times with DPBS, and fixed in 4% paraformaldehyde in DPBS for 10 min at room temperature. Slides were mounted in Prolong Gold Antifade with DAPI. Cells were imaged on a Zeiss LSM 510-META laser scanning confocal microscopy system.

For uptake analysis in primary epithelium, nasal epithelial cells were cultured from the nasal septum of C57BL/6N mice as previously described [30]. The following treatments were applied in duplicate at 300 μL per well, DQ-OVA only at 4 μg/mL in PBS, 0.05% NE with 4 μg/mL DQ-OVA in PBS, and a PBS only control. These were incubated at 37°C with 5% CO_2 for 2 h. Pelleted cells were resuspended and flow cytometry was performed using an Accuri C6. A total of 20,000 events were collected for each sample. The gating strategy was based on analysis in a side and forward scatter plot. In this plot, the dominant population (>95%) was analyzed for BODIPY-specific signal.

Detection of apoptosis and necrosis

To evaluate the induction of NE-driven apoptosis of nasal epithelium (a mixture of epithelial cells, connective tissues, and lymphocytes), C57BL6/N mice were nasally treated with 20% NE (15 μL). To determine if the NE mixture itself or its components do so, other mice were treated with either the equivalent concentration of CPC contained in 15 μL of 20% NE, with 20% W805E (a nonionic NE), or with sterile PBS. Nasal septal epithelium was harvested [30] and fixed in 10% buffered formalin for 24 h. Antigen retrieval was performed in DIVA decloacker buffer and blocked with peroxidase and Rodent block M (Biocare Medical) for 5 and 30 min, respectively according to manufacturer's recommendations. Tissues were stained with a 1:1000 dilution of pAb rabbit anti-Caspase-3 pAb (Cell Signaling) or with a 1:3000 dilution of rabbit pAb anticalreticulin (Abcam) for 1 h. Following wash, Rabbit-on-Rodent HRP-Polymer was applied for 30 min according to manufacturer guidelines. DAB chromogen was applied and the side was counterstained with Cat hematoxylin (Biocare medical).

Identification of cells dying by necrosis was characterized morphologically according to defined criteria [52]. In brief, necrotic cells were identified as cells containing dilated organelles and dissociated ribosomes from the endoplasmic reticulum. These cells do not contain pyknotic or fragmented nuclei and the degeneration proceeds without any detectable involvement of lysosomes. These experiments were performed twice with comparable results.

Epithelial gene expression analysis using microarrays

To evaluate regulation of NE-mediated changes in gene expression in nasal epithelial tissues, nasal septal epithelium was harvested immediately postmortem from CD-1 mice at either 6 h or 24 h following nasal treatment with either 20% NE (15 μL) or sterile PBS (15 μL). The tissue was collected in OTC and frozen by slow immersion in liquid nitrogen and stored at –80°C until used for microarray analysis. Total RNA was extracted per sample using RNeasy (Qiagen) according to the manufacturer's instructions. RNA samples were pooled and processed using an Ovation Biotin Labeling system from NuGen, Inc. following manufacturer's protocols. Prior to hybridization, the quality of RNA was accessed using an Agilent 2100 Bioanalyzer. Hybridization, detection, and scanning was performed using a mouse GeneChip® 430 2.0 manufactured by Affymetrix and a Affymetrix Scanner 3000 following manufactures guidelines. Gene expression values were calculated using a robust multiarray average (RMA) [53]. Complete microarray

data have been deposited in the public database Gene Expression Omnibus (GEO) under series accession number GSE25486 (http://www.ncbi.nlm.nih.gov/geo/query/acc.cgi). This assay was replicated for accuracy.

Analysis of cytokine and chemokine expression in BMDCs or in nasal septal tissues

BMDCs were cultured for 5 days as described above. A total of 4×10^6 BMDCs/treatment were stimulated with 0.001, 0.01, or 0.1% NE, 1, 10, or 30 μg/ml CT (List Laboratories). As a positive control BMDCs were treated also with 1 or 10 ng/ml LPS *Salmonella minnesota* (List Laboratories) or left untreated as negative control. The cells were stimulated in 2 mL/well of the medium with lowered content of FBS (2%) and mGM-CSF (1.5 ng/mL) at 37°C 5% CO_2 atmosphere for 24 h. Cytokine secretion was measured in supernatant using bead-based multiplex assay according to manufacturer protocol as described above (Millipore Multiplex 22).

Mucosal cytokines/chemokines were also analyzed in vivo. C57BL6/N mice ($n = 3$) were intranasally treated with 15 μL of 20% NE, 1 μg CT, or sterile PBS. Nasal septal epithelium was collected as above directly postmortem 18 h following treatment. The epithelium was manually homogenized using mortar and pestle and then gently digested using T-PER tissue extraction reagent (Thermo Scientific) according to manufacturer's recommendation. Cytokine secretion was measured in supernatant using bead-based multiplex assay according to manufacturer protocol as described above (Millipore Multiplex 22). Additionally, the supernatant was evaluated for the presence of TGF-β 1 and thymic stromal lymphopoietin (TLSP) via ELISA using a mouse/rat/porcine/canine TGF-ß1 immunoassay kit (Quantikine) and Mouse TSLP Immunoassay kit (Quantikine®) according to manufacturer's recommendations.

To evaluate the potential for NE to mediate cytokine expression in epithelial cells, 4×10^6 TC-1 cells were incubated with 0.001, 0.01, or 0.1% NE. The supernatant was evaluated using ELISA for TGF-β1, and TSLP as above. IL-6 was also measured using a custom ELISA. In brief, 96-well MaxiSorp® (Nunc) plates were coated with 2 μg/mL rabbit pAB anti-IL-6 (Abcam) and blocked with peroxidase. After washing, 100 μL of nondiluted supernatant/well was incubated on the plate for 2 h. After washing, 50 μL of a 1:200 dilution biotinylated anti-IL6 antibody (Abcam) was incubated in each well for 2 h. After washing, the plate was developed with streptavidin-HRP and read at an absorbance of 450 nm.

Immunization protocol for IL-6 mechanistic studies

For studies evaluating the role of IL-6, groups of IL-$6^{-/-}$ and WT (C57BL/6J) mice ($n = 5$) were i. n. immunized with 20 μg rPA ± 20% NE (12 μL), or sterile PBS (negative controls) on days 0 and 28. At week 6, the animals were euthanized and the spleens were immediately harvested and processed into a single cell suspension. rPA-specific in vitro recall responses were analyzed as previously described [24].

Statistical analysis

Statistical comparisons were assessed by two-way ANOVA with Tukey comparison, Student's *t*-test, and Mann-Whitney test by using GraphPad Prism version 5.00 (GraphPad Software, San Diego CA; www.graphpad.com). A p value < 0.05 was considered significant.

Acknowledgments: This project has been funded in part from the Bill and Melinda Gates Foundation, under award 37868 (PI Dr. Baker) and in part with Federal funds from the National Institute for Allergy and Infectious Disease, National Institutes of Health, Department of Health and Human Services, under Contract No. HHSN272200900031C (PI Dr. Baker). P. Makidon was supported by T32 RR07008 from National Center Research Resources of NIH. The authors would like to thank Dmitry Isakov, Pam Wong, Craig Johnson, Nick Mank, Guihua Jiang, Dotty Sorenson, Bruce Donohoe, Erby Wilkinson, Ingrid Bergin, and Paula Arrowsmith.

Conflict of Interest: Dr. James R. Baker Jr. holds an ownership stake in NanoBio, Corp., and is the inventor of technologies that the University has licensed to NanoBio, Corp. Some of these technologies are involved in this research, and NanoBio, Corp. is a subcontractor in this research to perform formulations. NanoBio, Corp. has no role in the study design of the work performed at UM, the data collection and analysis, the decision to publish, or the preparation of this manuscript.

References

1 **Ramanathan, M., Jr. and Lane, A. P.**, Innate immunity of the sinonasal cavity and its role in chronic rhinosinusitis. *Otolaryngol. Head Neck Surg.* 2007. **136:** 348–356.

2 **Isaacson, M. K., Juckem, L. K. and Compton, T.**, Virus entry and innate immune activation. *Curr. Top Microbiol. Immunol.* 2008. **325:** 85–100.

3 **Bomsel, M. and Alfsen, A.**, Entry of viruses through the epithelial barrier: pathogenic trickery. *Nat. Rev. Mol. Cell Biol.* 2003. **4:** 57–68.

4 **Joenvaara, S., Mattila, P., Renkonen, J., Makitie, A., Toppila-Salmi, S., Lehtonen, M., Salmi, et al.** Caveolar transport through nasal epithelium of birch pollen allergen Bet v 1 in allergic patients. *J. Allergy Clin. Immunol.* 2009. **124:** 135–142, e131–121.

5 **Ichinohe, T., Lee, H. K., Ogura, Y., Flavell, R. and Iwasaki, A.**, Inflammasome recognition of influenza virus is essential for adaptive immune responses. *J. Exp. Med.* 2009. **206:** 79–87.

6 **Kraehenbuhl, J. P. and Neutra, M. R.**, Epithelial M cells: differentiation and function. *Annu. Rev. Cell Dev. Biol.* 2000. **16:** 301–332.

7 **Fujimura, Y., Takeda, M., Ikai, H., Haruma, K., Akisada, T., Harada, T., Sakai, T. et al.**, The role of M cells of human nasopharyngeal lymphoid tissue in influenza virus sampling. *Virchows Arch.* 2004. **444:** 36–42.

8 **Spit, B. J., Hendriksen, E. G., Bruijntjes, J. P. and Kuper, C. F.**, Nasal lymphoid tissue in the rat. *Cell Tissue Res.* 1989. **255:** 193–198.

9 **Giannasca, P. J., Boden, J. A. and Monath, T. P.**, Targeted delivery of antigen to hamster nasal lymphoid tissue with M-cell-directed lectins. *Infect Immun.* 1997. **65:** 4288–4298.

10 **Chieppa, M., Rescigno, M., Huang, A. Y. and Germain, R. N.**, Dynamic imaging of dendritic cell extension into the small bowel lumen in response to epithelial cell TLR engagement. *J. Exp. Med.* 2006. **203:** 2841–2852.

11 **Neutra, M. R., Pringault, E. and Kraehenbuhl, J.-P.**, Antigen sampling across epithelial barriers and induction of mucosal immune responses. *Annu. Rev. Immunol.* 1996. **14:** 275–300.

12 **Borges, O., Lebre, F., Bento, D., Borchard, G. and Junginger, H. E.**, Mucosal vaccines: recent progress in understanding the natural barriers. *Pharm. Res.* 2010. **27:** 211–223.

13 **Belyakov, I. M., Kuznetsov, V. A., Kelsall, B., Klinman, D., Moniuszko, M., Lemon, M., Markham, P. D. et al.**, Impact of vaccine-induced mucosal high avidity CD8+ CTLs in delay of AIDS-viral dissemination from mucosa. *Blood* 2006. **107:** 3258–3264.

14 **Sui, Y., Zhu, Q., Gagnon, S., Dzutsev, A., Terabe, M., Vaccari, M., Venzon, D. et al.**, Innate and adaptive immune correlates of vaccine and adjuvant-induced control of mucosal transmission of SIV in macaques. *Proc. Natl. Acad. Sci. U.S.A.* 2010. **107:** 9843–9848.

15 **Didierlaurent, A. M., Morel, S., Lockman, L., Giannini, S. L., Bisteau, M., Carlsen, H., Kielland, A. et al.**, AS04, an aluminum salt- and TLR4 agonist-based adjuvant system, induces a transient localized innate immune response leading to enhanced adaptive immunity. *J. Immunol.* 2009. **183:** 6186–6197.

16 **Marinaro, M., Staats, H. F., Hiroi, T., Jackson, R. J., Coste, M., Boyaka, P. N., Okahashi, N. et al.**, Mucosal adjuvant effect of cholera toxin in mice results from induction of T helper 2 (Th2) cells and IL-4. *J. Immunol.* 1995. **155:** 4621–4629.

17 **van Ginkel, F. W., Jackson, R. J., Yoshino, N., Hagiwara, Y., Metzger, D. J., Connell, T. D., Vu, H. L. et al.**, Enterotoxin-based mucosal adjuvants alter antigen trafficking and induce inflammatory responses in the nasal tract. *Infect. Immun.* 2005. **73:** 6892–6902.

18 **Mutsch, M., Zhou, W., Rhodes, P., Bopp, M., Chen, R. T., Linder, T., Spyr, C. and Steffen, R.**, Use of the inactivated intranasal influenza vaccine and the risk of Bell's palsy in Switzerland. *N. Engl. J. Med.* 2004. **350:** 896–903.

19 **Sjoblom-Hallen, A., Marklund, U., Nerstedt, A., Schon, K., Ekman, L., Bergqvist, P., Lowenadler, B. et al.**, Gene expression profiling identifies STAT3 as a novel pathway for immunomodulation by cholera toxin adjuvant. *Mucosal. Immunol.* 2010. **3:** 374–386.

20 **Levine, M. M. and Sztein, M. B.**, Vaccine development strategies for improving immunization: the role of modern immunology. *Nat. Immunol.* 2004. **5:** 460–464.

21 **Shaffer, A. L., Rosenwald, A., Hurt, E. M., Giltnane, J. M., Lam, L. T., Pickeral, O. K. and Staudt, L. M.**, Signatures of the immune response. *Immunity* 2001. **15:** 375–385.

22 **Bielinska, A. U., Janczak, K. W., Landers, J. J., Markovitz, D. M., Montefiori, D. C. and Baker, J. R., Jr.**, Nasal immunization with a recombinant HIV gp120 and nanoemulsion adjuvant produces Th1 polarized responses and neutralizing antibodies to primary HIV type 1 isolates. *AIDS Res. Hum. Retroviruses* 2008. **24:** 271–281.

23 **Makidon, P. E., Bielinska, A. U., Nigavekar, S. S., Janczak, K. W., Knowlton, J., Scott, A. J., Mank, N. et al.**, Pre-clinical evaluation of a novel nanoemulsion-based hepatitis B mucosal vaccine. *PLoS ONE* 2008. **3:** e2954.

24 **Bielinska, A. U., Janczak, K. W., Landers, J. J., Makidon, P., Sower, L. E., Peterson, J. W. and Baker, J. R., Jr.**, Mucosal immunization with a novel nanoemulsion-based recombinant anthrax protective antigen vaccine protects against Bacillus anthracis spore challenge. *Infect. Immun.* 2007. **75:** 4020–4029.

25 **Bielinska, A. U., Chepurnov, A. A., Landers, J. J., Janczak, K. W., Chepurnova, T. S., Luker, G. D. and Baker, J. R., Jr.**, A novel, killed-virus nasal vaccinia virus vaccine. *Clin. Vaccine Immunol.* 2008. **15:** 348–358.

26 **Bielinska, A. U., Gerber, M., Blanco, L. P., Makidon, P. E., Janczak, K. W., Beer, M., Swanson, B. et al.**, Induction of Th17 cellular immunity with a novel nanoemulsion adjuvant. *Crit. Rev. Immunol.* 2010. **30:** 189–199.

27 **Asanuma, H., Thompson, A. H., Iwasaki, T., Sato, Y., Inaba, Y., Aizawa, C., Kurata, T. et al.**, Isolation and characterization of mouse nasal-associated lymphoid tissue. *J. Immunol. Methods* 1997. **202**: 123–131.

28 **Jovic, M., Sharma, M., Rahajeng, J. and Caplan, S.**, The early endosome: a busy sorting station for proteins at the crossroads. *Histol. Histopathol.* 2010. **25:** 99–112.

29 **Jones, B. A. and Gores, G. J.**, Physiology and pathophysiology of apoptosis in epithelial cells of the liver, pancreas, and intestine. *Am. J. Physiol.* 1997. **273:** G1174–1188.

30 **Antunes, M. B., Woodworth, B. A., Bhargave, G., Xiong, G., Aguilar, J. L., Ratner, A. J., Kreindler, J. L. et al.**, Murine nasal septa for respiratory epithelial air-liquid interface cultures. *Biotechniques* 2007. **43:** 195–196, 198, 200.

31 **Obeid, M., Panaretakis, T., Joza, N., Tufi, R., Tesniere, A., van Endert, P., Zitvogel, L. et al.**, Calreticulin exposure is required for the immunogenicity of gamma-irradiation and UVC light-induced apoptosis. *Cell Death Differ.* 2007. **14:** 1848–1850.

32 **McGeachy, M. J., Bak-Jensen, K. S., Chen, Y., Tato, C. M., Blumenschein, W., McClanahan, T. and Cua, D. J.**, TGF-beta and IL-6 drive the production of IL-17 and IL-10 by T cells and restrain T(H)-17 cell-mediated pathology. *Nat. Immunol.* 2007. **8:** 1390–1397.

33 **Vanden Bush, T. J., Buchta, C. M., Claudio, J. and Bishop, G. A.**, Cutting edge: importance of IL-6 and cooperation between innate and adaptive immune receptors in cellular vaccination with B lymphocytes. *J. Immunol.* 2009. **183:** 4833–4837.

34 **Myc, A., Kukowska-Latallo, J. F., Bielinska, A. U., Cao, P., Myc, P. P., Janczak, K., Sturm, T. R. et al.**, Development of immune response that protects mice from viral pneumonitis after a single intranasal immunization with influenza A virus and nanoemulsion. *Vaccine* 2003. **21:** 3801–3814.

35 **Makidon, P. E., Knowlton, J., Groom, J. V., 2nd, Blanco, L. P., LiPuma, J. J., Bielinska, A. U. and Baker, J. R., Jr.**, Induction of immune response to the 17 kDa OMPA Burkholderia cenocepacia polypeptide and protection against pulmonary infection in mice after nasal vaccination with an OMP nanoemulsion-based vaccine. *Med. Microbiol. Immunol.* 2010. **199**: 81–92.

36 **Pappenheimer, J. R. and Reiss, K. Z.**, Contribution of solvent drag through intercellular junctions to absorption of nutrients by the small intestine of the rat. *J. Membr. Biol.* 1987. **100:** 123–136.

37 **Madara, J. L. and Pappenheimer, J. R.**, Structural basis for physiological regulation of paracellular pathways in intestinal epithelia. *J. Membr. Biol.* 1987. **100:** 149–164.

38 **Marichal, T., Ohata, K., Bedoret, D., Mesnil, C., Sabatel, C., Kobiyama, K., Lekeux, P. et al.**, DNA released from dying host cells mediates aluminum adjuvant activity. *Nat. Med.* 2011. **17:** 996–1002.

39 **Kesimer, M., Scull, M., Brighton, B., DeMaria, G., Burns, K., O'Neal, W., Pickles, R. J. et al.**, Characterization of exosome-like vesicles released

from human tracheobronchial ciliated epithelium: a possible role in innate defense. *Faseb J.* 2009. **23:** 1858–1868.

40 **Van Niel, G., Mallegol, J., Bevilacqua, C., Candalh, C., Brugiere, S., Tomaskovic-Crook, E., Heath, J. K. et al.**, Intestinal epithelial exosomes carry MHC class II/peptides able to inform the immune system in mice. *Gut* 2003. **52:** 1690–1697.

41 **Nochi, T., Yuki, Y., Takahashi, H., Sawada, S., Mejima, M., Kohda, T., Harada, N. et al.**, Nanogel antigenic protein-delivery system for adjuvant-free intranasal vaccines. *Nat. Mater.* 2010. **9:** 572–578.

42 **Eisenbarth, S. C., Colegio, O. R., O'Connor, W., Sutterwala, F. S. and Flavell, R. A.**, Crucial role for the Nalp3 inflammasome in the immunostimulatory properties of aluminium adjuvants. *Nature* 2008. **453:** 1122–1126.

43 **van Duin, D., Medzhitov, R. and Shaw, A. C.**, Triggering TLR signaling in vaccination. *Trends Immunol.* 2006. **27:** 49–55.

44 **Lochner, M., Peduto, L., Cherrier, M., Sawa, S., Langa, F., Varona, R., Riethmacher, D. et al.**, In vivo equilibrium of proinflammatory IL-17+ and regulatory IL-10+ Foxp3+ RORgammat+ T cells. *J. Exp. Med.* 2008. **205:** 1381–1393.

45 **Bettelli, E., Korn, T. and Kuchroo, V. K.**, Th17: the third member of the effector T cell trilogy. *Curr. Opin. Immunol.* 2007. **19:** 652–657.

46 **Awasthi, A. and Kuchroo, V. K.**, Th17 cells: from precursors to players in inflammation and infection. *Int. Immunol.* 2009. **21:** 489–498.

47 **Pritts, T., Hungness, E., Wang, Q., Robb, B., Hershko, D. and Hasselgren, P. O.**, Mucosal and enterocyte IL-6 production during sepsis and endotoxemia–role of transcription factors and regulation by the stress response. *Am. J. Surg.* 2002. **183:** 372–383.

48 **Kida, H., Yoshida, M., Hoshino, S., Inoue, K., Yano, Y., Yanagita, M., Kumagai, T. et al.**, Protective effect of IL-6 on alveolar epithelial cell death induced by hydrogen peroxide. *Am. J. Physiol. Lung Cell Mol. Physiol.* 2005. **288:** L342–349.

49 **Lutz, M. B., Kukutsch, N., Ogilvie, A. L. J., Robner, S., Koch, F., Romani, N. and Schuler, G.**, An advanced culture method for generating large quantities of highly pure dendritic cells from mouse bone marrow. *J. Immunol. Methods* 1999. **223:** 77–92.

50 **Ballou, B., Ernst, L. A., Andreko, S., Harper, T., Fitzpatrick, J. A., Waggoner, A. S. and Bruchez, M. P.**, Sentinel lymph node imaging using quantum dots in mouse tumor models. *Bioconjug. Chem.* 2007. **18:** 389–396.

51 **Shapiro, F., Cahill, C., Malatantis, G. and Nayak, R. C.**, Transmission electron microscopic demonstration of vimentin in rat osteoblast and osteocyte cell bodies and processes using the immunogold technique. *Anat. Rec.* 1995. **241:** 39–48.

52 **Ziegler, U. and Groscurth, P.**, Morphological features of cell death. *News Physiol. Sci.* 2004. **19:** 124–128.

53 **Irizarry, R. A., Ooi, S. L., Wu, Z. and Boeke, J. D.**, Use of mixture models in a microarray-based screening procedure for detecting differentially represented yeast mutants. *Stat. Appl. Genet Mol. Biol.* 2003. **2**: Article 1.

Abbreviations: **BMDC**: bone marrow derived DC · **CT**: cholera toxin · **NE**: nanoemulsion

Full correspondence: Dr. Paul Makidon, Michigan Nanotechnology Institute for Medicine and Biological Sciences, University of Michigan, 3452 ARF, 1150 W. Medical Center Dr., Ann Arbor, Michigan 48892, USA
Fax: +1-734-936-2990
e-mail: pmakidon@umich.edu

Additional correspondence: Dr. James R. Baker, Jr., National Cancer Institute, Vaccine Branch, 10 Center Drive, Bldg 10, 6B-12, Bethesda, MD 20892, USA
e-mail: jbakerjr@umich.edu

Received: 19/12/2011
Revised: 13/4/2012
Accepted: 11/5/2012
Accepted article online: 1/6/2012

